Astrophys Space Sci (2009) 324: 219–223
DOI 10.1007/s10509-009-0110-y

ORIGINAL ARTICLE

2D hydrodynamic simulations of super star cluster winds in a bimodal regime

R. Wünsch · J. Palouš · G. Tenorio-Tagle · S. Silich

Received: 14 August 2009 / Accepted: 14 August 2009 / Published online: 3 September 2009

Abstract It is shown that the winds of very massive and compact clusters evolve in a special bimodal way, such that in which the material deposited by stars into the inner cluster region becomes thermally unstable, forms cold dense clumps, and eventually feeds further episodes of star formation, while the material deposited into the outer region creates a quasi-stationary wind. We perform 2D numerical simulations of such winds using the finite difference hydrodynamic code ZEUS for which the cooling routine has been modified to make it suitable for modelling extremely fast cooling regions. We explore how the fraction of the deposited mass which is accumulated inside the cluster depends on the cluster parameters.

Keywords Galaxies: star clusters · Stars: winds, outflows · ISM: kinematics and dynamics · Methods: numerical

1 Introduction

Super star clusters (hereafter SSCs) are observed in many starburst and interacting galaxies (Ho 1997; Whitmore 2006; Gilbert and Graham 2007), where they represent the dominant mode of star formation. They are young massive clusters consisting of typically 10^5–10^6 stars distributed in a spherical volume of radius 3–10 pc. The young massive stars deposit a substantial fraction of their mass (up to 30%) back into the ISM in the form of stellar winds and supernova explosions. Stellar synthesis models (see, for example Leitherer et al. 1999) predict that the total mechanical luminosity of such a cluster is $L_{\rm SC} \sim 10^{40}$–10^{41} erg s^{-1} during first several tens of Myr, assuming a Salpeter IMF. The stars are also powerful sources of ionizing radiation providing an approximately constant output of $\sim 10^{53}$ photons s^{-1} for the first 3 Myr, then dropping as $\sim t^{-5}$ (Tenorio-Tagle et al. 2005).

It has been suggested by Chevalier and Clegg (1985) that the mechanical energy of the mass deposited by stars is quickly thermalized in shock–shock collisions. The details of the thermalization process are unknown, however, it is assumed that the thermalized energy is partially radiated away immediately, and partially it heats the injected gas to very high temperatures ($\sim 10^6$–10^7 K). The later fraction is called the heating efficiency η and we assume that a reasonable value for it is between 0.1 and 1 (Wünsch et al. 2007). The hot medium is distributed almost homogeneously throughout the cluster volume, and since its pressure is much larger than the pressure of the surrounding ISM, it drives the star cluster wind. Neglecting radiative cooling, which is not important for smaller clusters, Chevalier and Clegg (1985) found a semi-analytical stationary solution for such a wind. Later, the adiabatic wind has also been studied numerically (see, e.g., Cantó et al. 2000; Raga et al. 2001).

However, it has been shown by Silich et al. (2004) that radiative cooling is important in the case of more massive and compact clusters. At first, it modifies the wind temperature outside the cluster—the wind cools down from $\sim 10^6$ K

R. Wünsch (✉)
Cardiff University, Queens Buildings, The Parade, Cardiff, CF24 3AA, UK
e-mail: richard@wunsch.cz

R. Wünsch · J. Palouš
Astronomical Institute, Academy of Sciences of the Czech Republic, Boční II 1401, 141 31 Prague, Czech Republic

G. Tenorio-Tagle · S. Silich
Instituto Nacional de Astrofísica Optica y Electrónica, AP 51, 72000 Puebla, México

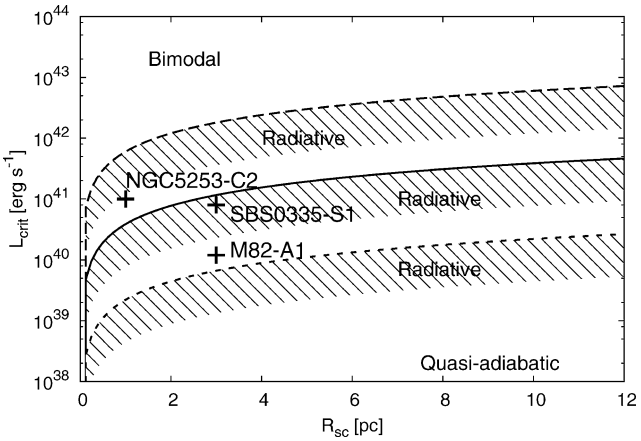

Fig. 1 The stationary solution of the wind can exist only below $L_{\rm crit}$ which is shown here as a function of the cluster radius $R_{\rm SC}$. The three $L_{\rm crit}$ lines for different values of the adiabatic terminal velocity $V_{\rm A,\infty} \equiv (2L_{\rm SC}/\dot{M}_{\rm SC})^{1/2}$ and heating efficiency η are shown ($\dot{M}_{\rm SC}$ is the total mass deposition rate). The *solid line* represents the parameters $V_{\rm A,\infty} = 1000$ km s^{-1}, $\eta = 1$; the *dashed line* $V_{\rm A,\infty} = 1500$ km s^{-1}, $\eta = 1$; and the *dotted line* $V_{\rm A,\infty} = 1000$ km s^{-1}, $\eta = 0.1$. The shaded areas denoted as "Radiative" are the regions where the stationary solution exists, but the cooling strongly modifies the wind temperature profile outside the cluster. Clusters above the threshold line evolve in the bimodal regime (see description in the text). The location of several massive SSCs with respect to the threshold lines are indicated by plus symbols (see Turner et al. 2003; Turner and Beck 2004; Thompson et al. 2006; Smith et al. 2006)

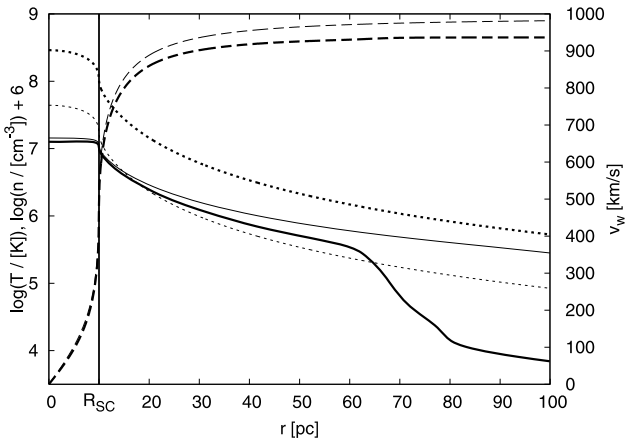

Fig. 2 The radial profiles of the temperature (*solid lines*), the particle density (*dotted lines*; note that units are m^{-3} to fit into the figure), and the velocity (*dashed lines*; belong to the right y-axis) obtained from the semi-analytical model. The *thin lines* represent the solution for the cluster with $L_{\rm SC} = 5 \times 10^{40}$ erg s^{-1} which behaves almost adiabatically, the *thick lines* show the solution for $L_{\rm SC} = 3 \times 10^{41}$ erg s^{-1} for which the wind cools down between 60 and 80 pc. The other cluster parameters are $R_{\rm SC} = 10$ pc and $V_{\rm A,\infty} = 1000$ km s^{-1}

to $\sim 10^4$ K at a certain radius (see Fig. 2). Furthermore, it turns out that the stationary solution cannot exist for even more massive and compact clusters. Figure 1 shows the critical luminosity ($L_{\rm crit}$) which separates the parameter space into two regions: the region below it where the stationary

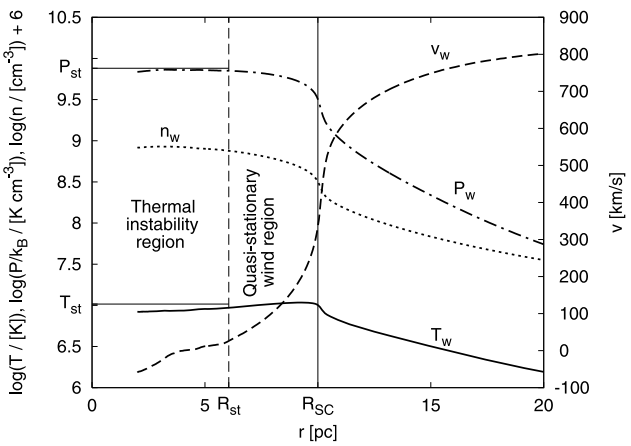

Fig. 3 The internal structure of the cluster in the bimodal regime. The cluster of radius $R_{\rm SC}$ is divided into two regions by the stagnation radius $R_{\rm st}$: the inner thermal instability region and the outer quasi-stationary wind region. The radial profiles of the wind particle density, temperature, pressure and radial velocity were obtained as the axial and time averages of the 2D simulation (the model with $L_{\rm SC} = 10^{42}$ erg s^{-1}) between 0.4 and 0.8 Myr. Only the hot gas ($T > 2 \times 10^4$) was taken into account. The values of the temperature and pressure at the stagnation radius obtained from the semi-analytical model are also shown

solutions exist, and the region above it where they are prohibited.

Based on 1D hydrodynamic simulations, the so called *bimodal solution* has been invented by Tenorio-Tagle et al. (2007) for the winds of clusters above $L_{\rm crit}$ line. The cluster is divided into two regions by the *stagnation radius* ($R_{\rm st}$) at which the wind radial velocity is zero. The outer region (between $R_{\rm st}$ and the cluster radius $R_{\rm SC}$) is able to accelerate the injected matter, while the mass in the central region becomes thermally unstable which leads to the drop of pressure there. The outer region can be described by a semi-analytical stationary solution, but the inner one is highly non-stationary and it has been suggested that warm clumps ($T \sim 10^4$ K) surrounded by a hot medium are formed there. Some of them may feed subsequent star formation, others may pass to the outer region, perturb the stationary wind there, and be ejected from the cluster. Therefore, the outer region is referred to as the quasi-stationary wind region, while the inner one is called the thermal instability region (see Fig. 3).

In this work we present the first 2D simulations that confirm the behavior predicted by the semi-analytical model and 1D simulations in Tenorio-Tagle et al. (2007). We also estimate the ratio of mass that leaves the cluster to the mass that stays there available for star formation.

2 Numerical code

We use the finite difference Eulerian hydrodynamic code ZEUS3D version 3.4.2. All calculations are carried out on

a spherical (r, θ) grid, symmetric along the ϕ-coordinate. We make use of the ability of ZEUS to work with non-equidistant grids and set the radial size of grid cells dr proportional to the radial coordinate r which ensures that the all grid cells are roughly regular ($dr \sim rd\theta$). Another advantage of the radially scaled grid is that the resolution is higher at smaller radii (inside the cluster) where the clumps are formed.

The cooling routine has been revised to make it suitable for the modelling of extremely fast cooling regions. In particular, the energy equation is solved by the Brent (1973) algorithm which is faster and more stable than the original Newton–Raphson method. Furthermore, the cooling rate has been included into the computation of the time-step. A common way of doing this is to limit the time-step so that the fraction of the internal energy that can be radiated away during one time-step must be smaller than some safety factor $\epsilon < 1$ (see, e.g., Suttner et al. 1997; where $\epsilon = 0.3$ was used). In this work we use $\epsilon = 0.25$. However, since this could lead to extremely small time-steps, which would substantially degrade the overall code performance, we do not allow the *global* time-step to decrease below 0.1 times the "hydrodynamic" time-step determined by the Courant–Friedrich–Levi criterion. In the case that a certain cell requires an even smaller time-step due to the cooling rate condition, we subdivide the time-step further and integrate the energy equation with the source terms only in the affected cell(s). This "time refinement" is applied only *locally*, so the CPU time is not wasted in cells where the high time resolution is not required.

In order to simulate the effect of the stellar radiation we do not allow the temperature to drop below $T_{\rm lim} = 10^4$ K. This is equivalent to the assumption that there are always enough UV photons to ionize the dense matter which would otherwise cool to much lower temperatures.

The wind source is modeled as a sphere into which energy and mass are continuously replenished at rates $L_{\rm SC}$ and $\dot{M}_{\rm SC}$, respectively. Note that in the text below we use the wind adiabatic terminal velocity $V_{\rm A,\infty} \equiv (2L_{\rm SC}/\dot{M}_{\rm SC})^{1/2}$ as a more convenient parameter instead of $\dot{M}_{\rm SC}$. The mass and energy deposition is homogeneous throughout the cluster volume with the rate densities $q_m = (3\dot{M}_{\rm SC})/(4\pi R_{\rm SC}^3)$ and $q_e = (3\dot{L}_{\rm SC})/(4\pi R_{\rm SC}^3)$. The following procedure is applied to each cell within the cluster volume at each time-step: (1) the density and the total energy in a given cell are saved to $\rho_{\rm old}$ and $e_{\rm tot,old}$; (2) new mass is inserted $\rho_{\rm new} = \rho_{\rm old} + A_{\rm noise}\zeta q_m dt$, and the velocity is corrected so that the momentum is conserved $\mathbf{v}_{\rm new} = \mathbf{v}_{\rm old}\rho_{\rm old}/\rho_{\rm new}$; (3) internal energy is corrected to conserve the total energy $e_{\rm i,mid} = e_{\rm tot,old} - \rho_{\rm new}\mathbf{v}_{\rm new}/2$; (4) the new energy is inserted in a form of internal energy $e_{\rm i,new} = A_{\rm noise}\zeta e_{\rm i,mid} + q_e dt$. ζ is a pseudo-random number in range $(-1, 1)$ generated each time it is used and $A_{\rm noise}$ is the relative amplitude of the noise. The inclusion of the noise is necessary to break the artificial spherical symmetry present in the initial conditions (see below). The model is very robust with respect to $A_{\rm noise}$—we have run tests with $A_{\rm noise} = 0.01, 0.05, 0.1$ and 0.5 and the general properties (mass fluxes at boundaries, number of fragments formed and their approximate sizes) of all of the models are practically the same, the only change is in the duration of the initial relaxation period during which the symmetry is lost. We use $A_{\rm noise} = 0.1$ for all the models described in this work.

The boundary conditions are set open at the both r-boundaries and periodic at the both θ-boundaries. The open inner r-boundary plays the role of a very simple star formation model—clumps which are born with inward velocities pass the inner boundary and disappear from the simulation. As the initial condition, the spherically symmetric stationary semi-analytical solution with $L_{\rm SC} = L_{\rm crit}$ is used.

3 Formation of warm dense clumps

Here we describe the typical behavior of the 2D model above the $L_{\rm crit}$ line. The cluster has parameters $R_{\rm SC} = 10$ pc, $V_{A,\infty} = 1000$ km s^{-1}, and $L_{\rm SC} = 10^{43}$ erg s^{-1} which places the cluster by factor of ~20 above the $L_{\rm crit}$ line in the parameter space. Note that the observed clusters have typically lower luminosities, however, they may reach the same $L_{\rm SC}/L_{\rm crit}$ ratios having the heating efficiency $\eta < 1$. For the sake of simplicity, we present only models with $\eta = 1$ in this work.

Figures 4, 5, 6, 7 show the state of the simulation at $t = 0.25$ Myr when equilibrium between the clump formation and ejection rate, on the one hand, and their passage rate through the inner boundary, on the other hand, is well established.

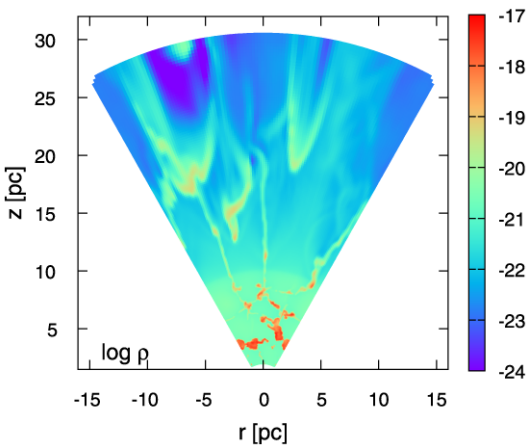

Fig. 4 The distribution of the density (in g cm^{-3}, logarithmic scale) across the computational domain at the time $t = 0.25$ Myr. The model parameters are $L_{\rm SC} = 10^{43}$ erg s^{-1}, $R_{\rm SC} = 10$ pc and $v_{\rm A,\infty} = 1000$ km s^{-1}

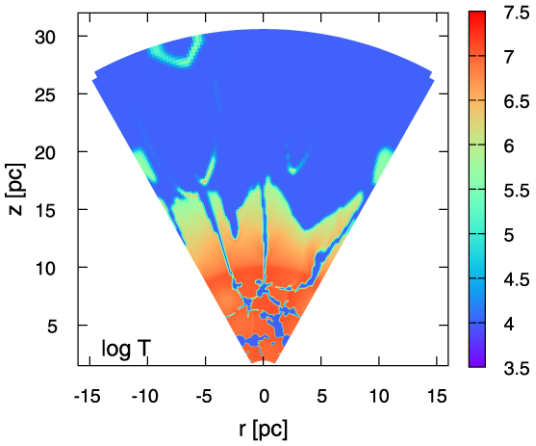

Fig. 5 The logarithm of the gas temperature (in K) at the same time and for the same model as in Fig. 4

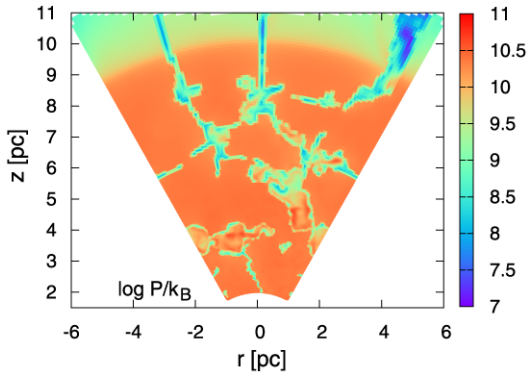

Fig. 6 The logarithm of the gas pressure in the star cluster at the same time and for the same model as in Fig. 4. The pressure is practically constant in the hot medium below $R_{\rm st}$, it has a lower value at the places which have just cooled down and at the clump boundaries where the material cools and flows to the clump surfaces. The pressure inside the well formed clumps is in equilibrium with its value in the hot medium (see, e.g., structures at $(-1, 3.5)$ pc and $(1, 4.5)$ pc)

The separation of the cluster into two regions can be seen in Fig. 7 which shows the wind velocity. The zero radial velocity surface which separates the outer region where the radial velocity is positive everywhere has a more complicated, non-spherical shape. Nevertheless, its average position stays close to the stagnation radius given in the semi-analytical approach by the formula semi-analytical approach (Wünsch et al. 2007) and denoted by the red arc in Fig. 7:

$$\frac{R_{\rm st}^3}{R_{\rm SC}^3} = 1 - \left(\frac{L_{\rm crit}}{L_{\rm SC}}\right)^{1/2}. \tag{1}$$

In the inner region, thermal instability occurs. The region which cools down is quickly compressed into a dense clump, by shocks propagating from its ambient hot high pressure medium. At the same time, the density in the ambient medium slightly decreases, because it expands into the

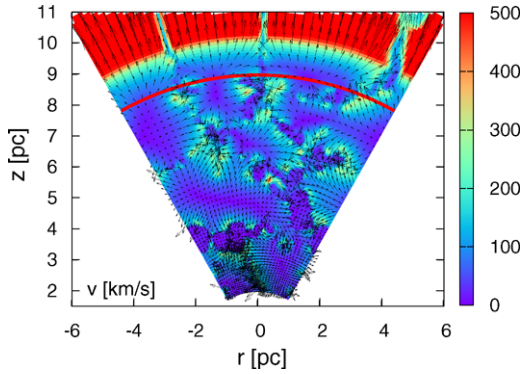

Fig. 7 The gas velocity represented by arrows and the color (magnitude in km s^{-1}) in the star cluster. The red arc shows the position of the stagnation radius $R_{\rm st}$ given by the semi-analytical solution. The time and the cluster parameters are the same as in Fig. 4

volume occupied previously by the cooled down matter. Another thermal instability may occur only after a while during which enough mass is accumulated there due to its continuous replenishment. By this mechanism, the hot medium inside the cluster is maintained in an equilibrium with the pressure almost constant everywhere below $R_{\rm st}$ (see Fig. 6) and close to the value given by the semi-analytical model (see Fig. 3)

$$P_{\rm st} = k_{\rm B} T_{\rm st} \frac{\mu_{\rm ion}}{\mu} \left[\frac{q_e - q_m a_{\rm st}^2/(\gamma - 1)}{\Lambda(T_{\rm st}, Z)}\right]^{1/2}, \tag{2}$$

where $T_{\rm st}$ is the temperature at the stagnation radius which has to be determined numerically (see Tenorio-Tagle et al. 2007), $c_{\rm st}$ and $\Lambda_{\rm st}$ are the corresponding sound speed and cooling function, respectively, μ and $\mu_{\rm ion}$ are the average particle and ion masses, respectively.

Figures 4 and 5 show the distribution of the density and temperature across the whole computational domain. We can see the clumps, some of them being ejected from the cluster and partially ablated by the surrounding wind.

4 Mass outflow from the cluster

In order to determine the fraction of the deposited mass that leaves the cluster and the fraction that stays inside it, we run several simulations with different cluster luminosities and measure the mass flux at the outer boundary of the computational domain during the period 0.4–0.8 Myr (chosen to omit the initial relaxation of the model). The results are summarized in Fig. 8 in which the fraction of outflowing mass is plotted as a function of $L_{\rm SC}/L_{\rm crit}$.

The outflow consists of two components: (1) the wind which is formed hot in the outer region of the cluster and cools down at some radius (in the presented simulation this occurs at ∼15 pc, see Fig. 5) and (2) the warm dense clumps

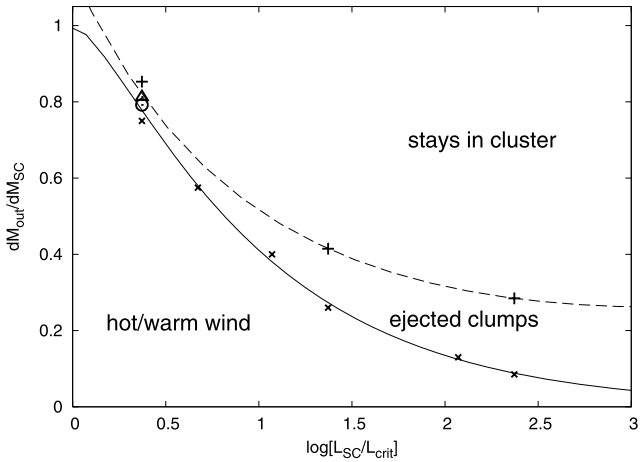

Fig. 8 The average mass flux measured at the outer boundary for several 1D and 2D simulations with different $L_{\rm SC}/L_{\rm crit}$ ratios. The $\times$ symbols denote the 1D simulations by Tenorio-Tagle et al. (2007). The 2D simulations are denoted by the other symbols depending on the resolution with which they were computed: 150×56 (*triangle*), 300×112 (*plus*), and 600×224 (*circle*). The 1D simulations follow the semi-analytical value for the fraction of mass which goes into the wind formed in the quasi-stationary wind region (denoted by *solid line*), because no clumps can be ejected if the artificial spherical symmetry is imposed. The *dashed line* is the fit to the mass fluxes of the 2D simulations. The difference between the two lines is mainly due to the ejected clumps which are present only in 2D simulations. The area above the dashed line represents the mass which stays inside the cluster

formed inside $R_{\rm st}$ that are able to leave the cluster. The simulations suggest that only a small fraction (up to $20\%\dot{M}_{\rm SC}$) of clumps is able to escape from the cluster—only the clumps which are born close to $R_{\rm st}$ are able to get above it and be ejected.

However, more simulations are required to check the dependence of this result on other parameters (e.g., the heating efficiency η). A more sophisticated model which includes a better model of star formation, the cluster gravity, the time evolution of the energy and mass deposition rates, etc., is also required.

Acknowledgements This study has been supported by project LC06014 Center for Theoretical Astrophysics of the Czech Ministry of Education and by CONACYT—México, research grant 47534-F and AYA2004-08260-CO3-O1 from the Spanish Consejo Superior de Investigaciones Científicas. R.W. acknowledges support by the Human Resources and Mobility Programme of the European Community under the contract MEIF-CT-2006-039802.

References

Brent, R.P.: Algorithms for Minimization Without Derivatives, Chap. 3. Prentice-Hall, Englewood Cliffs (1973)
Cantó, J., Raga, A.C., Rodríguez, L.F.: Astrophys. J. **536**, 896 (2000)
Chevalier, R.A., Clegg, A.W.: Nature **317**, 44 (1985)
Gilbert, A.M., Graham, J.R.: Astrophys. J. **668**, 168 (2007)
Ho, L.C.: In: Franco, J., Terlevich, R., Serrano, A. (eds.) Revista Mexicana de Astronomia y Astrofisica Conference Series, p. 5 (1997)
Leitherer, C., Schaerer, D., Goldader, J.D., Delgado, R.M.G., Robert, C., Kune, D.F., de Mello, D.F., Devost, D., Heckman, T.M.: Astrophys. J. Suppl. Ser. **123**, 3 (1999)
Raga, A.C., Velázquez, P.F., Cantó, J., Masciadri, E., Rodríguez, L.F.: Astrophys. J. Lett. **559**, L33 (2001)
Silich, S., Tenorio-Tagle, G., Rodríguez-González, A.: Astrophys. J. **610**, 226 (2004)
Smith, L.J., Westmoquette, M.S., Gallagher, J.S., O'Connell, R.W., Rosario, D.J., de Grijs, R.: Mon. Not. R. Astron. Soc. **370**, 513 (2006)
Suttner, G., Smith, M.D., Yorke, H.W., Zinnecker, H.: Astron. Astrophys. **318**, 595 (1997)
Tenorio-Tagle, G., Silich, S., Rodríguez-González, A., Muñoz-Tuñón, C.: Astrophys. J. **620**, 217 (2005)
Tenorio-Tagle, G., Wünsch, R., Silich, S., Palouš, J.: Astrophys. J. **658**, 1196 (2007)
Thompson, R.I., Sauvage, M., Kennicutt, R.C. Jr., Engelbracht, C.W., Vanzi, L.: Astrophys. J. **638**, 176 (2006)
Turner, J.L., Beck, S.C.: Astrophys. J. Lett. **602**, L85 (2004)
Turner, J.L., Beck, S.C., Crosthwaite, L.P., Larkin, J.E., McLean, I.S., Meier, D.S.: Nature **423**, 621 (2003)
Whitmore, B.C.: In: Livio, M., Villaver, E. (eds.) Massive Stars: From Pop III and GRBs to the Milky Way. Cambridge University Press, Cambridge (2006) (in preparation). arXiv:astro-ph/0612695
Wünsch, R., Silich, S., Palouš, J., Tenorio-Tagle, G.: Astron. Astrophys. **471**, 579 (2007)